Mechanism of Microsomal Triglyceride Transfer Protein Catalyzed Lipid Transport†

Amy Atzel‡,§ and John R. Wetterau*,‖

Division of Lipoprotein Research, Department of Pharmacology and Cell Biophysics, University of Cincinnati College of Medicine, Cincinnati, Ohio 45267-0575, and Department of Metabolic Diseases, Bristol-Myers Squibb, Princeton, New Jersey 08543-4000

Received April 8, 1993; Revised Manuscript Received July 2, 1993•

ABSTRACT: The microsomal triglyceride transfer protein (MTP) is found in the lumen of microsomes isolated from liver and intestine. This protein, which catalyzes the transport of neutral lipids between membranes, appears to play an important role in the biogenesis of plasma very low density lipoproteins and chylomicrons. Enzyme kinetic studies were used to investigate the mechanism of MTP-catalyzed lipid transport. Initial rates of [^{14}C]triolein and [^{14}C]cholesteryl oleate transport from donor to acceptor small unilamellar vesicles were determined at varying donor and acceptor membrane concentrations. Results using two different kinetic analyses demonstrated lipid transport was best described by ping-pong bi-bi kinetics, indicating that MTP is a lipid binding protein which shuttles triglyceride and cholesteryl ester molecules between membranes. This model for lipid transport was supported by a fluorescent lipid binding assay in which MTP was able to extract pyrene-labeled cholesteryl ester from a vesicle. MTP–membrane interactions and lipid transport were regulated by membrane surface charge. Equilibrium gel filtration chromatography demonstrated MTP has a higher affinity for neutrally charged membranes than negatively charged membranes. In agreement with the membrane binding studies, MTP-mediated lipid transfer was inhibited by increasing the concentration of negatively charged phospholipid molecules in donor membranes.

The microsomal triglyceride transfer protein (MTP)[1] catalyzes the transport of triglyceride (TG), cholesteryl ester (CE), and phosphatidylcholine (PC) between membranes (Wetterau & Zilversmit, 1984). MTP activity is found within the lumen of microsomes isolated from the liver and intestinal mucosa (Wetterau & Zilversmit, 1986). Purified MTP from bovine liver is a soluble heterodimer consisting of 88- and 58-kDa subunits noncovalently associated (Wetterau & Zilversmit, 1985; Wetterau et al., 1990, 1991a). The 58-kDa component has been identified as the multifunctional protein, protein disulfide isomerase (Wetterau et al., 1990). The dimeric structure and subcellular location of MTP make it unique among lipid transfer proteins. Most other mammalian intracellular lipid transfer proteins have been isolated from the postmicrosomal supernatant (cytosol) of various tissues [reviewed in Helmkamp (1986) and Rueckert (1990)]. All are monomeric proteins with molecular masses in the range of 8–35 kDa. MTP is also distinct from the monomeric 58–74-kDa plasma cholesteryl ester transfer protein (CETP) (Ihm et al., 1982a; Morton & Zilversmit, 1982; Albers et al., 1984; Hesler et al., 1987), which is a glycoprotein containing a 52-kDa polypeptide backbone (Drayna et al., 1987). CETP, like MTP, catalyzes the transport of CE, TG, and PC.

The tissue distribution, intracellular location, and catalytic activity of MTP have led to the hypothesis that it plays a role in the synthesis of very low density lipoproteins (VLDL) and chylomicrons (Wetterau et al., 1986). The recent finding that MTP was not detectable in subjects with the genetic disease abetalipoproteinemia supports this hypothesis (Wetterau et al., 1992). Several reports have suggested that plasma VLDL are assembled by the sequential addition of lipid to nascent particles (Higgins & Hutson, 1984; Bõstrom et al., 1988; Janero & Lane, 1983). Major unresolved issues regarding the assembly of these lipoproteins include how and where the major structural protein apolipoprotein B (apo B) initially becomes associated with lipid to form a soluble particle and how nascent VLDL particles become enriched with triglyceride. MTP may play an important role in either one or both of these processes. However, before we can understand how MTP is involved in lipoprotein biogenesis, it is important to elucidate the mechanism by which MTP transports lipids between membranes. This will provide a framework for understanding the molecular events involved in lipoprotein assembly.

Protein-catalyzed lipid transport can occur via several mechanisms. In a shuttle mechanism, the transfer protein binds to a donor membrane and extracts a lipid molecule(s). The transfer protein containing the bound lipid then dissociates from the membrane and diffuses to a second membrane where it binds and deposits the lipid molecule(s). The cytosolic PC-specific (van den Besselaar et al., 1975) and phosphatidylinositol (Helmkamp et al., 1976) transfer proteins utilize this mechanism. In a ternary complex mechanism, the transfer protein binds two substrate membranes simultaneously, forming a transient ternary complex which allows exchange of lipid to occur. Kinetic modeling of CETP-mediated lipid transport supports this mechanism (Ihm et al., 1982b), although alternate models have been proposed (Barter & Jones

† This work was supported in part by grants from the National Institutes of Health (HL 40993) and the Bristol-Myers Squibb Pharmaceutical Research Institute.

* To whom correspondence should be addressed.
‡ University of Cincinnati College of Medicine.
§ Supported by an Albert J. Ryan fellowship.
‖ Bristol-Myers Squibb.

• Abstract published in *Advance ACS Abstracts*, September 15, 1993.

[1] Abbreviations: MTP, microsomal transfer protein or microsomal triglyceride transfer protein; TG, triglyceride; CE, cholesteryl ester; PC, phosphatidylcholine; DPPC, dipalmitoylphosphatidylcholine; pyrene-CE, cholesteryl 1-pyrenedecanoate; [ACC], concentration of acceptor vesicles; [DON], concentration of donor vesicles; v, initial velocity; VLDL, very low density lipoproteins; SUV, small unilamellar vesicles; ER, endoplasmic reticulum; CETP, cholesteryl ester transfer protein; apo B, apolipoprotein B; BSA, bovine serum albumin.

1980; Swenson et al., 1988). The cytosolic nonspecific lipid transfer protein appears to operate by yet another mechanism (Nichols & Pagano, 1983; Gadella & Wirtz, 1991). This protein penetrates the surface of the membrane and enhances spontaneous polar lipid transfer by enabling lipid molecules to exit the membrane more readily. Although this latter mechanism may be reasonable for the transport of phospholipids and polar sterols, it is unlikely that such a mechanism would be feasible for the transport of insoluble triglycerides and cholesteryl esters. The goal of this study is to determine the mechanism of MTP-catalyzed lipid transport.

MATERIALS AND METHODS

Materials. Triolein, egg phosphatidylcholine, cholesteryl oleate, cardiolipin, and fatty acid free bovine serum albumin (BSA) were purchased from Sigma (St. Louis, MO). Egg phosphatidic acid, semisynthetic (Na^+ salt), was purchased from Matraya, Inc. (Pleasant Gap, PA). The [*carboxyl*-^{14}C]triolein (114 mCi/mmol), [*oleate*-1-^{14}C]cholesteryl oleate (52 mCi/mmol), and [2-*palmitoyl*-9,10-^{3}H(N)]dipalmitoylphosphatidylcholine (50 Ci/mmol) were purchased from New England Nuclear (Hoffman Estates, IL). Cholesteryl 1-pyrenedecanoate was purchased from Molecular Probes (Eugene, OR). All lipids were stored under N_2 gas in chloroform at −20 °C.

Isolation of MTP. MTP was purified from bovine liver as originally described (Wetterau & Zilversmit, 1985) and subsequently modified (Wetterau et al., 1991b). Purified MTP was dialyzed into 15 mM Tris, pH 7.4, 40 mM NaCl, 1 mM ethylenediaminetetraacetate, and 0.02% NaN_3 buffer (hereafter referred to as assay buffer), assayed for protein with the Pierce BCA reagent (Rockford, IL), and stored at 4 °C. BSA (1 mg/mL) was added to dilute MTP solutions to stabilize the protein.

Preparation of Donor and Acceptor Membranes. Donor and acceptor PC vesicles containing either TG or CE were prepared as follows. In all kinetic studies, except otherwise indicated, donor membranes contained egg PC, 0.25 mol % [^{14}C]triolein or 0.25 mol % [^{14}C]cholesteryl oleate, and 5 mol % cardiolipin to confer a net negative charge, while acceptor membranes contained egg PC, a trace of [^{3}H]dipalmitoylphosphatidylcholine ([^{3}H]DPPC), and 0.25 mol % unlabeled triolein or cholesteryl oleate. Unilamellar phospholipid vesicles were prepared by bath sonication (Laboratory Supplies Co. Inc., Hicksville, NY) under a nitrogen atmosphere at room temperature. Following sonication, the heterogeneous unilamellar vesicles were fractionated by ultracentrifugation using a modification of the procedure described by Barenholz et al. (1977) to obtain a homogeneous population of small unilamellar vesicles (SUV). Sonicated vesicles in 6 mL of assay buffer were spun at 159000*g* for 2 h in a Beckman (Palo Alto, CA) Ti50.3 rotor. The SUV contained in the top 4 mL of the centrifuge tube were removed by pipet. Typically, 45–65% of the original lipid was recovered in this fraction. The bottom 2 mL and pellet, which contained large unilamellar and multilamellar vesicles, respectively, were discarded. Purified vesicles were utilized in experiments within 5 h of preparation.

Aliquots of SUV were characterized by fractionation on a Bio-Gel A15-M gel permeation column (fractionation range 40 000 to 15 × 10^6) (Bio-Rad, Richmond, CA) to ensure purity of the vesicle preparation. SUV homogeneity was confirmed by incorporating both [^{14}C]triolein and [^{3}H]DPPC into vesicles and demonstrating that the ^{3}H/^{14}C ratio across the Bio-Gel A15-M peak of the purified vesicles was constant.

Lipid Transfer Assay. TG and CE transfer was measured from donor to acceptor SUV in an assay similar to that previously described by Wetterau and Zilversmit (1985). Donor membranes, acceptor membranes, 100 ng (0.7 pmol) of MTP, and 5 mg of BSA were adjusted to a total volume of 0.5 mL of assay buffer and incubated at 23 °C for 30 and 60 min. Transfer reactions were terminated by addition of 0.5 mL of DEAE (Whatman DE-52) suspension (1:1 ratio of DEAE:15 mM Tris, pH 7.4), which binds the negatively charged donor membranes. DEAE-bound donors were then pelleted by centrifugation at 15000*g* for 2 min. The [^{14}C]-triolein or [^{14}C]cholesteryl oleate in an aliquot of the supernatant was measured by scintillation counting. Appearance of ^{14}C-TG or ^{14}C-CE in the supernatant represents transfer of labeled neutral lipid from donor to acceptor membranes. Nonspecific lipid transfer (less than 1%) and nonprecipitated donor membranes (less than 2% as determined in control experiments) were measured as lipid transfer in the absence of MTP and subtracted from the total ^{14}C-labeled neutral lipid in the supernatant to calculate the rate of protein-stimulated lipid transfer. Because [^{3}H]DPPC transfer is insignificant relative to ^{14}C-TG or ^{14}C-CE transfer in this assay [CE and TG are transferred 30–50 times faster than PC; see Wetterau and Zilversmit (1985)], [^{3}H]DPPC was used as an indicator of acceptor vesicle recovery in the supernatant. The high recovery of [^{3}H]DPPC (ranged from 95% to 105%) confirms that PC transfer was insignificant. A 5% variation in acceptor vesicle recovery would have minimal effects on the calculated transfer rate.

To calculate the total neutral lipid transfer, first-order kinetics were used ($x_t = x_0e^{-kt}$, where x_0 and x_t equal the fraction of labeled lipid in the donor membrane at times 0 and t, respectively; ktX_0 = mass lipid transfered, where X_0 equals the initial mass of labeled lipid in the donor membrane). This corrects for the dilution of radiolabeled lipid in the donor SUV which results from the transfer of unlabeled lipid from acceptor to donor SUV. The results were expressed as velocities, graphed in double-reciprocal format ($1/v$ versus 1/[DON]), and curve fitted by linear regression.

Experimental Design. To evaluate the kinetic mechanism for TG and CE transport, two different experimental approaches were used. Both approaches account for acceptor membrane inhibition which was experimentally observed (for example, see Figure 3, where TG transfer decreases with increased concentration of acceptor vesicles). Donor membrane inhibition which would result in a nonlinear (concave upward at low 1/[DON]) double-reciprical plot was never observed. Ping-pong bi-bi kinetics are diagnostic of a shuttle mechanism, and random bi-bi kinetics are diagnostic of a ternary complex mechanism for MTP-catalyzed lipid transport (Figure 1).

(*A*) *Approach 1.* Initial velocity (v) measurements were made at varying donor membrane concentrations ([DON]) (25–400 pmol/mL) expressed as picomoles of TG or CE per milliliter, while acceptor membrane concentrations ([ACC]) were held constant. Experiments were then repeated at several [ACC] (4–1000 pmol/mL). The results were plotted as $1/v$ versus 1/[DON] to generate a series of lines which can be compared to the patterns predicted from the equations for the kinetic mechanisms: eq 1 for ping-pong bi-bi kinetics modified for acceptor–acceptor membrane inhibition (Segel, 1975a) and eq 2 for random bi-bi kinetics modified for acceptor membrane inhibition [derived from rapid equilibrium as-

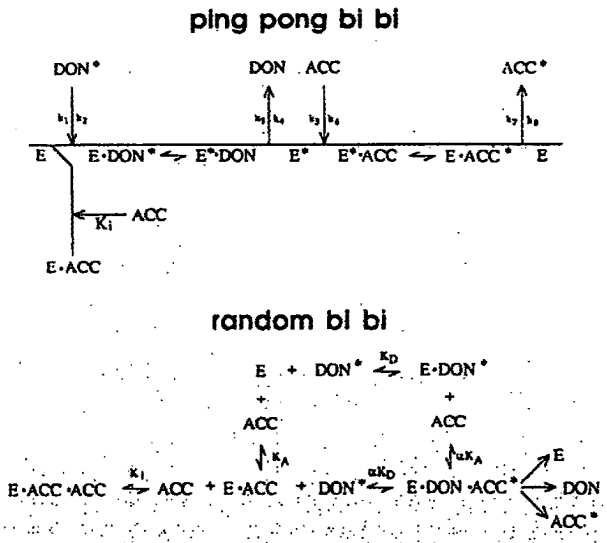

FIGURE 1: Ping-pong bi-bi (shuttle) and random bi-bi (ternary complex) mechanisms. In the ping-pong bi-bi mechanism (top), K_D and K_A are steady-state constants equal to $k_7(k_2 + k_3)/k_1(k_3 + k_7)$ and $k_3(k_6 + k_7)/k_5(k_3 + k_7)$ respectively, and K_i is the dissociation constant for the MTP–ACC complex. In the random bi-bi mechanism (bottom) K_D, K_A, αK_D, αK_A, and K_i are equal to [E][DON]/[E·DON], [E][ACC]/[E·ACC], [E·ACC][DON]/[E·DON·ACC], [E·DON]·[ACC]/[E·DON·ACC], and [E·ACC][ACC]/[E·ACC·ACC], respectively. Abbreviations: E = enzyme, DON = donor membranes, ACC = acceptor membranes, and * = TG or CE.

sumptions as outlined in Segel (1975b)].

ping-pong bi-bi kinetics

$$\frac{1}{v} = \frac{1}{[\mathrm{DON}]}\left[\frac{K_D(1 + [\mathrm{ACC}]/K_i)}{V_{max}}\right] + \frac{1}{V_{max}}\left(1 + \frac{K_A}{[\mathrm{ACC}]}\right) \quad (1)$$

random bi-bi kinetics

$$\frac{1}{v} = \frac{1}{[\mathrm{DON}]}\left[\frac{\alpha K_D(1 + [\mathrm{ACC}]/K_i + K_A/[\mathrm{ACC}])}{V_{max}}\right] + \frac{1}{V_{max}}\left(1 + \frac{\alpha K_A}{[\mathrm{ACC}]}\right) \quad (2)$$

In both mechanisms, at high [ACC], acceptor membranes behave as competitive inhibitors, and a series of nonparallel intersecting lines result. The slopes of the intersecting lines increase with increasing [ACC] in a counterclockwise manner ($[\mathrm{ACC}]/K_i$ term dominates slope). At low [ACC] (in the absence of acceptor membrane inhibition), $[\mathrm{ACC}]/K_i$ becomes insignificant, and this term does not influence the slope. In this case, ping-pong bi-bi kinetics generates a series of parallel lines, while random bi-bi kinetics generates a series of intersecting lines with the slopes of the lines decreasing with increasing [ACC].

(*B*) *Approach 2.* In the second kinetic approach, [DON] was set equal to [ACC], and both substrates were varied simultaneously in a 1:1 ratio. Initial velocities were measured as a function of substrate concentration. Actual concentrations of DON and ACC ranged from 2 to 1200 pmol of TG or CE/mL. Because [DON] is equal to [ACC], the donor term can be substituted for the acceptor term, and eqs 1 and 2 reduce to eqs 3 and 4 for ping-pong bi-bi and random bi-bi kinetics, respectively.

ping-pong bi-bi kinetics

$$\frac{1}{v} = \frac{1}{[\mathrm{DON}]}\left(\frac{K_D + K_A}{V_{max}}\right) + \frac{1}{V_{max}}\left(1 + \frac{K_D}{K_i}\right) \quad (3)$$

random bi-bi kinetics

$$\frac{1}{v} = \frac{1}{[\mathrm{DON}]}\left(\frac{\alpha K_D + \alpha K_A}{V_{max}}\right) + \frac{\alpha K_D K_A}{[\mathrm{DON}]^2 V_{max}} + \frac{1}{V_{max}}\left(1 + \frac{\alpha K_D}{K_i}\right) \quad (4)$$

There are no variables in the intercept or slope term of eq 3 so a double-reciprocal plot yields a straight line. Equation 4 is different from eq 3 in that the $[\mathrm{DON}]^2$ term in the denominator causes the double-reciprocal plot to be parabolic (concave up) at low [DON] (Rudolph & Fromm, 1979). When substrate concentrations become very high, however, the term containing $[\mathrm{DON}]^2$ will approach zero, and the double-reciprocal plot will be similar to that of eq 3. A beneficial aspect of this second approach is that the shape of the double-reciprocal plots is not affected by acceptor competitive inhibition as occurs with the first approach. K_i appears only in the intercept term in both eqs 3 and 4 and thus does not influence the shape of the curve.

Equilibrium Gel Filtration Chromatography. To estimate the affinity of MTP for substrates, equilibrium gel filtration chromatography was performed. Donor and acceptor vesicles were perpared and purified as described above. A Sephacryl S-300 column (Pharmacia, Piscataway, NJ) (1 × 27 cm) was equilibrated with assay buffer alone or assay buffer containing 250 pmol of TG/mL of substrate vesicles. MTP (0.5 μg in 10 mg of BSA) was loaded onto the column, and its elution volume was measured in the absence or presence of vesicles in the elution buffer. The elution positions for vesicles and MTP were determined by measuring radioactivity and lipid transfer activity, respectively. A shift in the elution position of MTP in the presence of vesicles is indicative of MTP binding to vesicles.

The dissociation constants (K_D) for MTP–vesicle complexes were estimated from the shift in the elution position of MTP using the relationship $K_D = [\mathrm{MTP}][\mathrm{VES}]/[\mathrm{MTP\text{–}VES}]$, where [MTP] equals the fraction of the elution time MTP is free, [MTP–VES] equals the fraction of the elution time MTP is bound to vesicles, and [VES] equals the free vesicle concentration. Under experimental conditions, the total vesicle concentration was 10 times that of MTP, assuming 3000 PC molecules per vesicle (Huang & Mason, 1978). Therefore, free [VES] was not significantly different from total [VES] (250 pmol of TG/mL), and the latter value was used in the calculations.

Fluorescent Lipid Transfer Assay. PC vesicles containing 6 mol % cholesteryl 1-pyrenedecanoate were prepared by sonication as described above except the vesicles were not isolated by centrifugation following sonication. At this concentration in the membrane, pyrene-CE is self-quenched. The fluorescence intensity of the vesicles (0.36 nmol of CE in 0.8 mL of assay buffer) was measured at 380 nm (excitation 340 nm) in a Perkin-Elmer luminescence spectrometer LS 50B (Norwalk, CT). Excitation and emission slit widths were set to 2.5 nm, and the temperature was maintained at 23 °C. MTP (0.47 nmol) in 100 μL of assay buffer was added, and the time-dependent change in fluorescence intensity was measured. As a control, the change in fluorescence of the vesicles in the absence of MTP was measured following the addition of assay buffer.

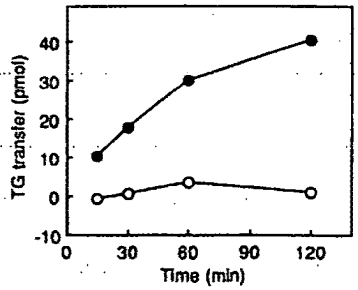

FIGURE 2: Bidirectional and unidirectional lipid transport. Lipid transport was investigated by measuring the apparent TG transfer over time in the presence of 100 ng of MTP. Donor membranes (300 pmol of TG/mL) contained 0.25% ^{14}C-TG, while acceptor membranes (300 pmol of TG/mL) contained either 0.25% ^{14}C-TG (open circles) or no TG (120 nmol/mL phosphatidylcholine) (solid circles).

RESULTS

Assay Conditions. Preliminary experiments were performed to establish conditions for measuring initial velocities. At 23 °C, with 200 ng/mL or less MTP, triglyceride transfer was linear with time for 60 min at all donor concentrations used (data not shown). With more than 400 ng/mL MTP, or incubation times longer than 60 min, transfer versus time deviated from linearity. Generally, this corresponded to greater than 30% transfer. All kinetic experiments were performed at 23 °C with 200 ng/mL (1.3 pmol/mL) MTP. Under these conditions, 30% transfer was not exceeded.

Lipid transfer proteins may promote the exchange (bidirectional movement) or the net transfer (unidirectional movement) of lipid molecules between membranes. In our transfer assays, the initial TG concentration was 0.25 mol % in both donor (radiolabeled TG) and acceptor (unlabeled TG) membranes. To determine whether MTP promoted exchange or net transfer of TG, the unlabeled TG in acceptor vesicles was replaced with ^{14}C-TG, and the apparent time-dependent transfer of ^{14}C-TG was measured. If ^{14}C-TG exchange occurs, the ^{14}C-TG in each vesicle population would remain constant, regardless of MTP-catalyzed lipid transport. However, if net transfer occurs, one vesicle population would become enriched in ^{14}C-TG while the other would become depleted. When radiolabeled TG was incorporated into both donor and acceptor membranes, there was no time-dependent change in the ^{14}C-TG content in acceptor membranes as indicated by the absence of apparent TG transfer (Figure 2). This demonstrates that MTP catalyzes ^{14}C-TG exchange under these experimental conditions. Identical results (data not shown) were obtained with CE transport. In subsequent analyses, first-order kinetics were used (see Materials and Methods) to calculate the total TG or CE transfer. This corrects for the dilution of labeled lipid in the donor particles resulting from lipid exchange. When TG was omitted from acceptor vesicles, unidirectional transport of TG from donor to acceptor membranes was observed (Figure 2).

Mechanism of MTP-Mediated Lipid Transport. Two different kinetic approaches were employed to determine the mechanism of MTP-catalyzed lipid transport. In the first approach, the donor membrane concentration was varied while the acceptor membrane concentration was held constant. This was then repeated at varying acceptor membrane concentrations. In the second approach, donor and acceptor membrane concentrations were set equal to each other and varied simultaneously in a 1:1 ratio. Each of these approaches exhibits characteristic double-reciprocal plots that can be utilized to diagnose the kinetic mechanism as outlined in Materials and Methods.

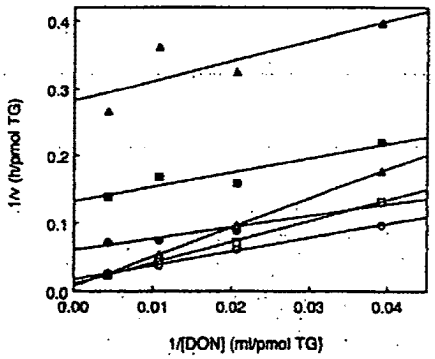

FIGURE 3: Double-reciprocal plot—approach 1. Plot of $1/v$ versus $1/[DON]$ at varying acceptor membrane concentrations. Data points are an average of two initial velocity measurements. Acceptor concentations were 4 (solid triangles), 10 (solid squares), 22 (solid circles), 90 (open circles), 220 (open squares), and 436 (open triangles) pmol of TG/mL. Data points were fit to lines by linear regression.

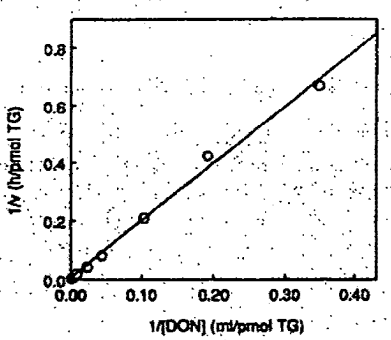

FIGURE 4: Double-reciprocal plot—approach 2. Plot of $1/v$ versus $1/[DON]$ when [DON] = [ACC]. TG transfer was measured as a function of substrate concentration. Data points are an average of two initial velocity measurements. Data points were fit to a line by linear regression (r = 0.997; y intercept = 0.0050).

Results of approach 1 are shown in Figure 3. Acceptor concentrations above 100 pmol of TG/mL result in a series of intersecting lines with decreasing slopes with decreasing [ACC]. This is diagnostic of acceptor membrane inhibition for both the ping-pong bi-bi and random bi-bi mechanisms. The change in slope is caused by competitive inhibition by acceptor membranes as [ACC] becomes significant relative to K_i. At low [ACC], the double-reciprocal plot yields a series of lines that appear parallel, with the $1/v$ intercepts decreasing with increasing [ACC]. These results are consistent with a ping-pong mechanism; however, mechanism diagnosis using this approach is difficult because of the limited range of [ACC] which can be used. At high [ACC], there is substrate inhibition, and at low [ACC], it is difficult to obtain accurate transfer rates. Similar results were found for cholesteryl ester transfer (data not shown).

Results of kinetic analysis by approach 2, in which [DON] = [ACC] and both are varied simultaneously, are shown in Figure 4. The double-reciprocal plot is a straight line which is diagnostic of ping-pong bi-bi kinetics (eq 3). Similar results were obtained in two additional experiments performed with TG and three experiments performed with CE (data not shown). In eq 3, K_i only influences the intercept, so a straight line results regardless of substrate inhibition. If lipid transport occurred by a ternary complex mechanism, the data would have fit a parabola (eq 4) significantly better than a straight line (eq 3) (Mannervik, 1982). The data were fit to the generic equations $1/y = a + b(1/x)$ and $1/y = a + b(1/x) + c(1/x)^2$ for a straight line and parabola, respectively. The parabolic solution gave an equation with a negative coefficient for $(1/$

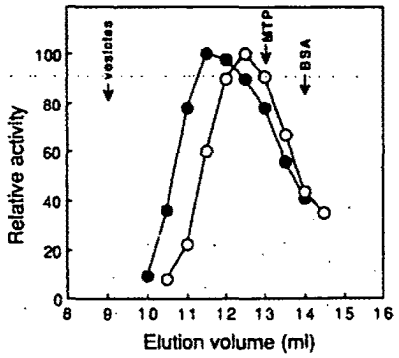

FIGURE 5: MTP binding to donor and acceptor membranes. A Sephacryl S-300 column (1 × 27 cm) was equilibrated in assay buffer, and the elution of MTP (0.5 μg) was measured in the absence or presence of 250 pmol of TG/mL of donor membranes (open circles) or acceptor membranes (solid circles) in the elution buffer. The elution peaks of donor or acceptor vesicles alone, MTP alone, and a BSA standard are indicated by arrows.

$x)^2$: $1/y = -0.0034 + 2.33(1/x) - 1.15(1/x)^2$, $r = 0.998$, causing it to be similar to the straight line solution of $1/y = 0.0049 + 1.96(1/x)$, $r = 0.997$. For mechanism diagnosis, the simpler model (eq 3, ping-pong bi-bi kinetics) was chosen over the more complex model since one fit was not significantly better than the other (Mannervik, 1982).

Affinity of MTP for Donor and Acceptor Membranes. The affinity of MTP for substrate vesicles was investigated by equilibrium gel filtration chromatography. The elution position of MTP was measured on a Sephacryl S-300 column equilibrated in assay buffer or assay buffer containing 250 pmol of TG/mL of donor or acceptor vesicles (Figure 5). The elution of MTP was shifted to earlier fractions in the presence of either donor or acceptor vesicles, indicating that MTP binds to both vesicles. The affinity of MTP for acceptor membranes, however, is higher than its affinity for donor membranes as indicated by the larger shift in the elution position of MTP in the presence of acceptors. The estimated dissociation constants (see Materials and Methods) for MTP–donor and MTP–acceptor vesicle complexes are 1800 pmol of TG/mL and 400 pmol of TG/mL, respectively. The higher affinity for neutral acceptor vesicles compared to negatively charged donor vesicles agrees with the observed substrate inhibition at high concentrations of acceptors, while no such effect was observed with donors.

The ability of cardiolipin (a negatively charged phospholipid) to decrease the affinity of MTP for vesicles suggests that MTP-catalyzed lipid transport may be regulated by membrane charge. To test this hypothesis, increasing concentrations of cardiolipin were incorporated into donor vesicles, and the the effect upon TG transfer was determined. Figure 6 shows that as the content of cardiolipin in donor membranes increases, the TG transfer rate decreases. Similar results were observed when phosphatidic acid replaced cardiolipin as the negatively charged phospholipid (data not shown).

Lipid Binding Properties of MTP. Protein-mediated lipid transfer by a shuttle mechanism indicates that the lipid molecules are bound to the protein as they are transported. To investigate the lipid molecule binding properties of MTP, a fluorescent assay was used to measure the time-dependent binding of neutral lipid to MTP. PC vesicles containing 6 mol % pyrene-CE were prepared by sonication. The fluorescence of pyrene-CE at 380 nm is dependent upon its concentration in the membrane (Wetterau et al., 1991b). At 6 mol %, it is self-quenched. Pyrene-CE binding to MTP will be evident by an increase in fluorescence upon addition of

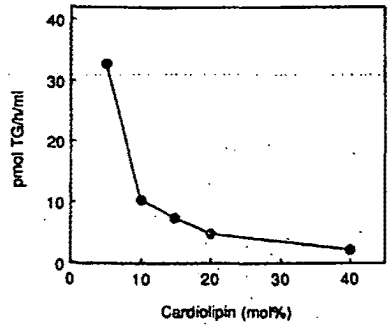

FIGURE 6: Membrane charge regulates lipid transfer. Vesicles were prepared as described in Materials and Methods except that they were not fractionated by centrifugation. Cardiolipin content of the donor vesicles was varied as shown. TG transfer in the presence of 200 ng/mL MTP was measured at 23 °C in assay buffer. Spontaneous lipid transfer (absence of MTP) was less than 2% of the total.

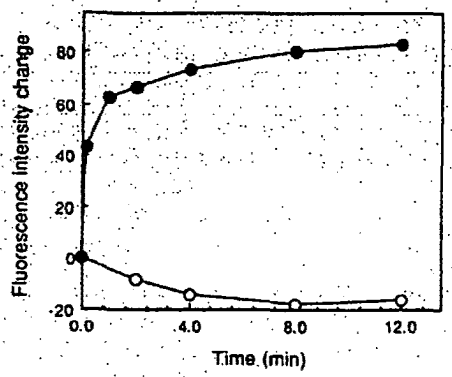

FIGURE 7: Time course of pyrene-CE binding to MTP. MTP, 0.47 nmol (solid circles), or assay buffer (open circles) was added to vesicles containing 0.36 nmol of pyrene-CE, and the time-dependent change in fluorescence was measured at 23 °C. Excitation and emission wavelengths were 340 and 380 nm, respectively. The initial fluorescence intensity was 237.

MTP to pyrene-CE vesicles, which indicates that pyrene-CE is removed from its self-quenched environment. Figure 7 shows that when MTP is added to vesicles, a rapid increase in fluorescence is observed. Thus, MTP binds pyrene-labeled cholesteryl ester.

DISCUSSION

Two independent kinetic approaches were used to demonstrate that MTP-catalyzed lipid transport is best described by ping-pong bi-bi kinetics, which indicates that MTP shuttles lipid molecules between membranes. Substrate inhibition complicated the analysis. In approach 1, at high concentrations of acceptor vesicles, both ping-pong bi-bi and random bi-bi mechanisms exhibit increasing slopes with increasing [ACC] in a double-reciprocal plot. This occurs because [ACC] is significant relative to K_i, thus affecting the slope terms of eqs 1 and 2. To diagnose the kinetic mechanism by this approach, [ACC] needs to be insignificant compared to K_i. However, if [ACC] is too low, accurate transfer rates cannot be determined. The first approach yielded a series of lines which appeared parallel (Figure 3) at [ACC] < 100 pmol/mL, consistent with ping-pong bi-bi kinetics. In this model, K_i is the dissociation constant of an acceptor–MTP complex. At [ACC] greater than 100 pmol/mL, [ACC] is significant relative to K_i and substrate inhibition is observed, which is in agreement with the K_i predicted from a direct measure of the MTP–acceptor vesicle dissociation constant (400 pmol/mL) by equilibrium gel filtration.

DOCKET ALARM

Explore Litigation Insights

Docket Alarm provides insights to develop a more informed litigation strategy and the peace of mind of knowing you're on top of things.

Real-Time Litigation Alerts

Keep your litigation team up-to-date with **real-time alerts** and advanced team management tools built for the enterprise, all while greatly reducing PACER spend.

Our comprehensive service means we can handle Federal, State, and Administrative courts across the country.

Advanced Docket Research

With over 230 million records, Docket Alarm's cloud-native docket research platform finds what other services can't. Coverage includes Federal, State, plus PTAB, TTAB, ITC and NLRB decisions, all in one place.

Identify arguments that have been successful in the past with full text, pinpoint searching. Link to case law cited within any court document via Fastcase.

Analytics At Your Fingertips

Learn what happened the last time a particular judge, opposing counsel or company faced cases similar to yours.

Advanced out-of-the-box PTAB and TTAB analytics are always at your fingertips.

API

Docket Alarm offers a powerful API (application programming interface) to developers that want to integrate case filings into their apps.

LAW FIRMS
Build custom dashboards for your attorneys and clients with live data direct from the court.

Automate many repetitive legal tasks like conflict checks, document management, and marketing.

FINANCIAL INSTITUTIONS
Litigation and bankruptcy checks for companies and debtors.

E-DISCOVERY AND LEGAL VENDORS
Sync your system to PACER to automate legal marketing.